Redox Biology 14 (2018) 142–153

Contents lists available at ScienceDirect

Redox Biology

journal homepage: www.elsevier.com/locate/redox

Research Paper

IDH2 deficiency increases the liver susceptibility to ischemia-reperfusion injury via increased mitochondrial oxidative injury

Sang Jun Han[a], Hong Seok Choi[a], Jee In Kim[b], Jeen-Woo Park[c], Kwon Moo Park[a,*]

[a] Department of Anatomy, Cardiovascular Research Institute and BK21 Plus, Kyungpook National University School of Medicine, 680 Gukchaebosang-ro, Junggu, Daegu 41944, Republic of Korea
[b] Department of Molecular Medicine and MRC, College of Medicine, Keimyung University, 1095 Dalgubeol-daero 250-gil, Dalseogu, Daegu 42601, Republic of Korea
[c] School of Life Sciences and Biotechnology, College of Natural Sciences, Kyungpook National University, 80 Daehak-ro, Bukgu, Daegu 41566, Republic of Korea

ARTICLE INFO

Keywords:
Liver ischemia
Mitochondria
Oxidative stress
Apoptosis
IDH2

ABSTRACT

Mitochondrial $NADP^+$-dependent isocitrate dehydrogenase 2 (IDH2) is a major producer of mitochondrial NADPH, required for glutathione (GSH)-associated mitochondrial antioxidant systems including glutathione peroxidase (GPx) and glutathione reductase (GR). Here, we investigated the role of IDH2 in hepatic ischemia-reperfusion (HIR)-associated mitochondrial injury using *Idh2*-knockout (*Idh2*$^{-/-}$) mice and wild-type (*Idh2*$^{+/+}$) littermates. Mice were subjected to either 60 min of partial liver ischemia or sham-operation. Some mice were administered with 2-(2,2,6,6-tetramethylpiperidin-1-oxyl-4-ylamino)-2-oxoethyl) triphenylphosphonium chloride (mito-TEMPO, a mitochondria-targeting antioxidant). HIR induced severe histological and functional damages of liver in both *Idh2*$^{+/+}$ mice and *Idh2*$^{-/-}$ mice and those damages were more severe in *Idh2*$^{-/-}$ mice than in wild-type littermates. HIR induces dysfunction of IDH2, leading to the decreases of NADPH level and mitochondrial GR and GPx functions, consequently resulting in mitochondrial and cellular oxidative injury as reflected by mitochondrial cristae loss, mitochondrial fragmentation, shift in mitochondrial fission, cytochrome c release, and cell death. These HIR-induced changes were greater in *Idh2*$^{-/-}$ mice than wild-type mice. The mito-TEMPO supplement significantly attenuated the aforementioned changes, and these attenuations were much greater in *Idh2*$^{-/-}$ mice when compared with wild-type littermates. Taken together, results have demonstrated that HIR impairs in the IDH2-NADPH-GSH mitochondrial antioxidant system, resulting in increased mitochondrial oxidative damage and dysfunction, suggesting that IDH2 plays a critical role in mitochondrial redox balance and HIR-induced impairment of IDH2 function is associated with the pathogenesis of ischemia-reperfusion-induced liver failure.

1. Introduction

Hepatic ischemia-reperfusion injury (HIRI) is a key factor in the postoperative dysfunction of the liver and is a common clinical problem [1]. Studies have demonstrated that oxidation of intracellular molecules including proteins, lipids, and DNA, cause oxidative injury to various intracellular organelles eventually leading to cell death [1–5]. Among intracellular organelles, mitochondria are a major producer of reactive oxygen species (ROS), and are simultaneously a primary target of oxidative stress. Under normal conditions, mitochondrial redox status is balanced by mitochondrial antioxidant systems including manganese superoxide dismutase (MnSOD), glutathione peroxidase (GPx), and thioredoxin (Trx)/peroxiredoxin (Prx). However, pathological conditions such as ischemia-reperfusion induce dysfunction in these mitochondrial antioxidant systems, leading to the oxidation of mitochondrial entities and the subsequent mitochondrial dysfunction, structural disruption, and the activation of the intrinsic apoptosis pathway. Indeed, apoptosis is known to be a major form of cell death caused by HIRI [6]. However, the role of the mitochondrial antioxidant systems in HIR-induced liver injury remains to be defined.

Glutathione is an important antioxidant in animals. Reduced glutathione (GSH) is capable of preventing oxidative damage to cellular components by directly neutralized free radicals and reactive oxygen compounds. In the mitochondrion, H_2O_2 generated from superoxide by MnSOD is continuously converted to H_2O by GSH. During this process, GSH is oxidized form of oxidized glutathione (GSSG). This GSSG is recycled by glutathione reductase (GR) to form GSH, which can then continue in the H_2O_2 removing process [7,8]. For the reduction of GSSG by GR, NADPH is required. Indeed, recent studies have demonstrated that mitochondrial NADPH levels are highly correlated with

* Correspondence to: Department of Anatomy, Kyungpook National University School of Medicine, 680 Gukchaebosang-ro, Junggu, Daegu 41944, Republic of Korea.
E-mail address: kmpark@knu.ac.kr (K.M. Park).

http://dx.doi.org/10.1016/j.redox.2017.09.003
Received 19 August 2017; Received in revised form 31 August 2017; Accepted 6 September 2017
Available online 08 September 2017

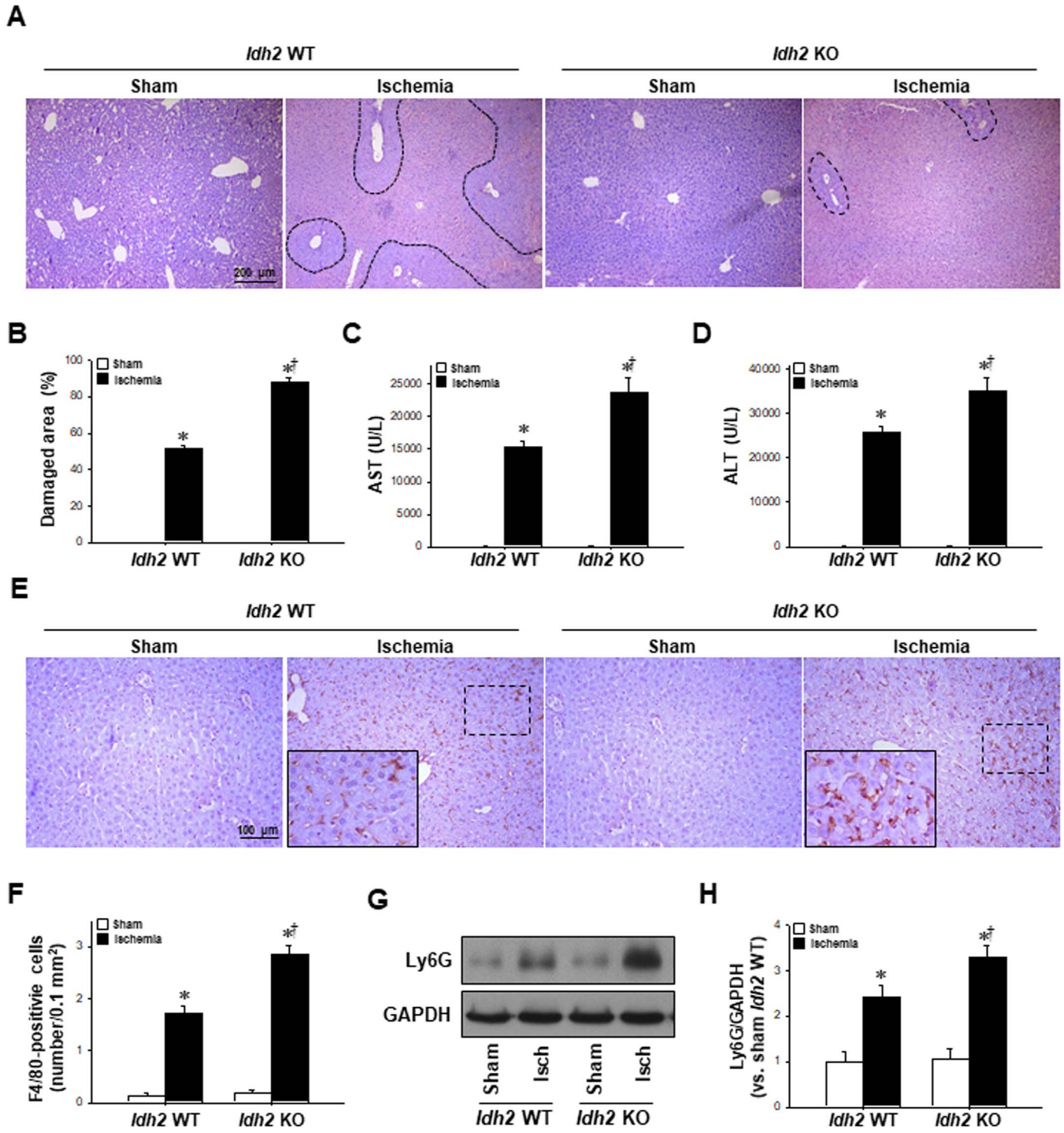

Fig. 1. Histological and functional damages to the liver of *Idh2*$^{+/+}$ and *Idh2*$^{-/-}$ mice after HIR. Livers were harvested 5 h after surgery. Liver sections were stained with PAS reagent (A) and the damaged area (B) were determined. Plasma concentrations of AST (C) and ALT (D) were measured. (E) Liver sections were subjected to immunohistochemical staining using an anti-F4/80 antibody. Hematoxylin was used to stain the nuclei. (F) F4/80-positive cells were counted. (G) Whole liver lysates were subjected to western blot analysis using an anti-Ly6G antibody. GAPDH was used as a loading control. (H) The densities of the Ly6G bands on the blot were determined using ImageJ software. The results are expressed as the means ± SEM (n = 6). *, $p < 0.05$ vs. sham-operated *Idh2*$^{+/+}$. †, $p < 0.05$ vs. ischemia-operated *Idh2*$^{+/+}$. IDH2, NADP$^+$-dependent isocitrate dehydrogenase 2; AST, Aspartate aminotransferase; ALT, Alanine aminotransferase; GAPDH, glyceraldehyde-3-phosphate dehydrogenase; PAS, Periodic acid–Schiff.

mitochondrial oxidative stress, which causes the dysfunction and structural damage to mitochondria [8,9]. Therefore, because neither NADPH nor GSH can penetrate the inner membrane of mitochondria [8,10,11], the NADPH producing system in the mitochondria may play a very important role in mitochondrial oxidative stress-related injuries including ischemia-reperfusion injury.

Isocitrate dehydrogenase 2 (IDH2) is localized in mitochondria and reduces NADP$^+$ to NADPH during the decarboxylation of isocitrate to α-ketoglutarate [9,10]. Given this reaction, IDH2 is recognized as a key generator of NADPH in mitochondria [9,10]. Recent studies have demonstrated that IDH2 is a critical for the maintenance of mitochondrial redox balance [9,12–15]. Therefore, in this study, we investigated

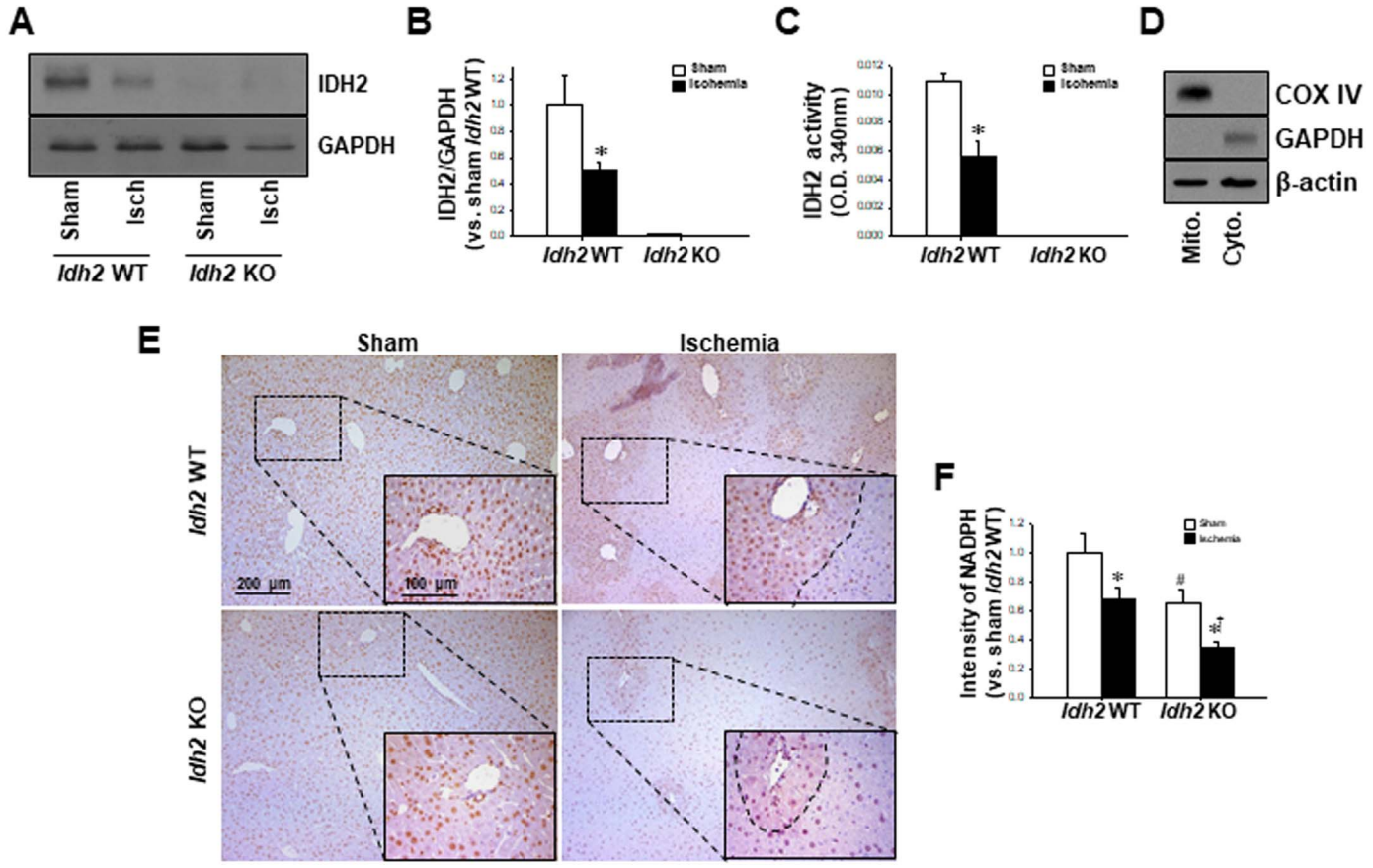

Fig. 2. Changes in IDH2 expression and activity, and NADPH levels in the *Idh2*$^{+/+}$ and *Idh2*$^{-/-}$ mice livers after HIR. Livers were harvested 5 h after surgery. (A, B) Whole liver lysates were subjected to western blot analysis using anti-IDH2 antibodies. GAPDH was used as a loading control. (B) The densities of the IDH2 bands on the blot were determined using ImageJ software. (C) The enzyme activity of IDH2 was measured in the liver mitochondrial fractions. (D) The mitochondrial (Mito) and cytosolic (Cyto) fractions were isolated and the efficient separation of the fractions was confirmed by western blot analysis using anti-COX IV and GAPDH antibodies, respectively. β-actin was used as the loading control. (E) Liver sections were subjected to immunohistochemical staining using an anti-NADPH antibody. (F) The intensity of NADPH staining was measured using i-solution software. The results are expressed as the mean ± SEM (n = 6). *, P < 0.05 vs. respective sham-operated mice. #, p < 0.05 vs. sham-operated *Idh2*$^{+/+}$. †, p < 0.05 vs. ischemia-operated *Idh2*$^{+/+}$. IDH2, mitochondrial NADP$^+$-dependent isocitrate dehydrogenase 2.

whether IDH2 is involved in the HIR-induced liver injury. Here, we report, for the first time, that HIR induces IDH2 dysfunction along with a reduction of mitochondrial NADPH levels and that *Idh2* gene deletion exacerbates HIR-induced mitochondrial oxidative injury and liver cell death. These results suggest that IDH2 could be a potential target for therapeutics against HIR-induced liver failure.

2. Materials and methods

2.1. Animal preparation

All experiments were conducted using 8- to 10-week-old male *Idh2* knockout (*Idh2*$^{-/-}$) and wild-type (*Idh2*$^{+/+}$) littermates weighing 22–24 g [16]. The study was conducted in accordance with the guidelines of the Institutional Animal Care and Use Committee of Kyungpook National University, Republic of Korea, and in accordance with the Guide for the Care and Use of Laboratory Animals published by the US National Institutes of Health (NIH Publication No. 85–23, revised 2011). The mice were provided with free access to water and standard chow. Some mice were treated with 2-(2,2,6,6-tetramethylpiperidin-1-oxyl-4-ylamino)-2-oxoethyl) triphenylphosphonium chloride (mito-TEMPO [17], 5 mg/kg body weight; Sigma, St. Louis, MO), via intraperitoneal (i.p.) injection, twice, at 17 h and 1 h before surgery. The mice were anesthetized by i.p. injection of sodium pentobarbital (50 mg/kg body weight; Sigma) before surgery. Partial liver ischemia was performed by occlusion of the portal triad for 60 min. Briefly, the mouse abdomen was opened using scissors, beginning at the mid-abdomen and ending at the xiphoid process. The intestines were removed gently from the abdominal cavity onto moistened sterilized gauze using a moistened cotton swab to expose the portal triad (portal vein, hepatic artery, and bile duct). The portal triad was clamped with a non-traumatic microaneurysm clamp (Roboz Surgical Instruments, Washington D.C., WA) after adding 50 μL of 1000 U/mL heparin. After clamping, 500 μL of 10 U/mL heparinized-saline was added to the clamped portal triad. Liver ischemia was confirmed visually by the change in the liver color from reddish brown to cream. To protect fluid loss during surgery, sterilized gauze was put on the retracted intestines and 500 μL of sterilized saline was added to the gauze. After 60 min of ischemia, the clamp was removed carefully and 500 μL of saline was added to the abdominal cavity. The intestines were replaced in the abdominal cavity following reperfusion. Reperfusion was confirmed visually by observing the liver color return to reddish brown. The muscle layer and skin were sutured with 5-0 silk. Body temperature was maintained at 36.5–37 °C throughout all the surgical procedures using a temperature-controlled heating device (FHC, Bowdoin, ME). A sham surgery was performed that was equivalent to the operation for ischemia except that the portal triad was not clamped. The ischemic lobes were excised 5 h after surgery and were either snap-frozen in liquid nitrogen for western blot analysis or perfusion-fixed in PLP (4% paraformaldehyde, 75 mM L-lysine, and 10 mM sodium periodate; Sigma) for histological studies.

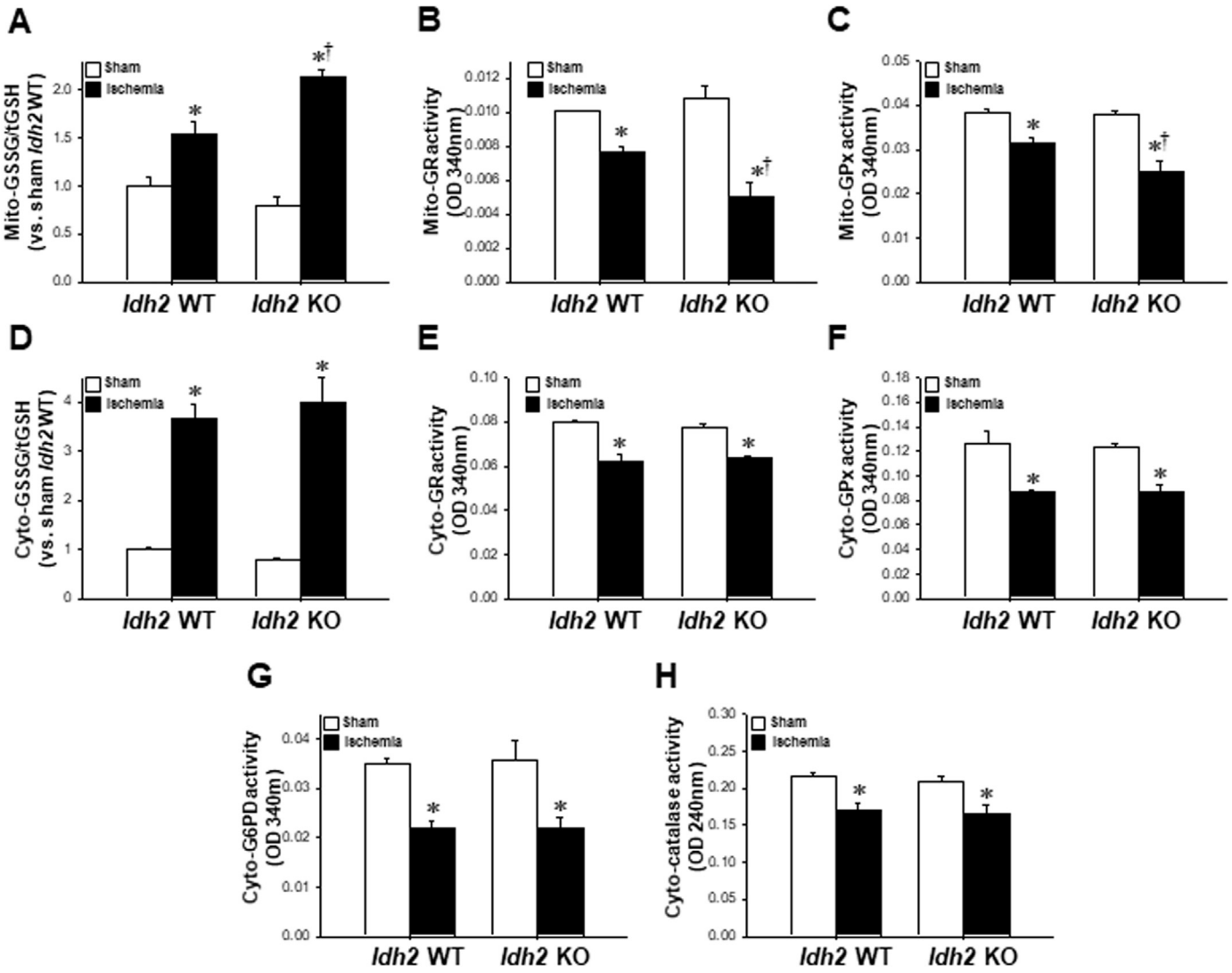

Fig. 3. The ratio of GSSG to total glutathione and the activities of glutathione reductase (GR), glutathione peroxidase (GPx), glucose-6-phosphate dehydrogenase (G6PD), and catalase in the *Idh2*$^{+/+}$ and *Idh2*$^{-/-}$ mouse livers after HIR. Livers were harvested 5 h after surgery. In the liver mitochondrial (Mito) fractions, the ratio of GSSG to total glutathione (GSSG/tGSH) (A), and the activities of GR (B), and GPx (C) were determined. In the liver cytosolic (Cyto) fractions, the ratio of GSSG to total glutathione (GSSG/tGSH) (D), and the activities of GR (E), and GPx (F), G6PD (G), and catalase (H) were determined. The results are expressed as the mean ± SEM (n = 6). *, P < 0.05 vs. respective sham-operated mice. #, p < 0.05 vs. sham-operated *Idh2*$^{+/+}$. †, p < 0.05 vs. ischemia-operated *Idh2*$^{+/+}$. IDH2, mitochondrial NADP$^+$-dependent isocitrate dehydrogenase 2; GSSG, oxidized glutathione; tGSH, total glutathione.

2.2. Histology

Liver paraffin sections were stained with Periodic acid–Schiff (PAS) stain according to a standard protocol. To score hepatocyte morphological damage, the injured areas were determined in five fields per liver.

2.3. Western blot analysis

Western blotting was performed as described previously [18]. Western blots were performed using the following antibodies; IDH2 [9], Ly6G (eBioscience, San Diego, CA), COX IV (Cell Signaling, Danvers, MA), Optic atrophy 1 (Opa1; BD bioscience, San Diego, CA), Fission 1 (Fis1; Sigma), Bax (EMD Millipore, Billerica, MA), Bcl-2 (EMD Millipore), Bcl-xL (BD bioscience), cleaved caspase-3 (Cell Signaling), β-actin (Sigma), and glyceraldehyde-3-phosphate dehydrogenase (GAPDH; NOVUS, Littleton, CO) antibodies.

2.4. Immunohistochemical staining

Immunohistochemical staining was performed using anti-NADPH (1:100; Biorbyt, Cambridge, UK), anti-8-hydroxy-2′-deoxyguanosine (8-OHdG; Abcam, Cambridge, MA), and anti-F4/80 (Serotec, Oxford, UK) antibodies, as described previously [19].

2.5. Measurement of hydrogen peroxide and lipid peroxidation in the liver

Hydrogen peroxide levels in liver tissues were measured using the ferric sensitive dye, xylenol orange, as described previously [20]. To determine the extent of lipid peroxidation, thiobarbituric acid-reactive substances (TBARS, Sigma) were used as described previously [21].

2.6. Preparation of cytosolic and mitochondrial fractions

Cytosolic and mitochondrial fractions were prepared as described previously [22]. These fractions were confirmed by western blotting using antibodies against GAPDH for the cytosolic fraction and COX IV for the mitochondrial fraction (Fig. 3C).

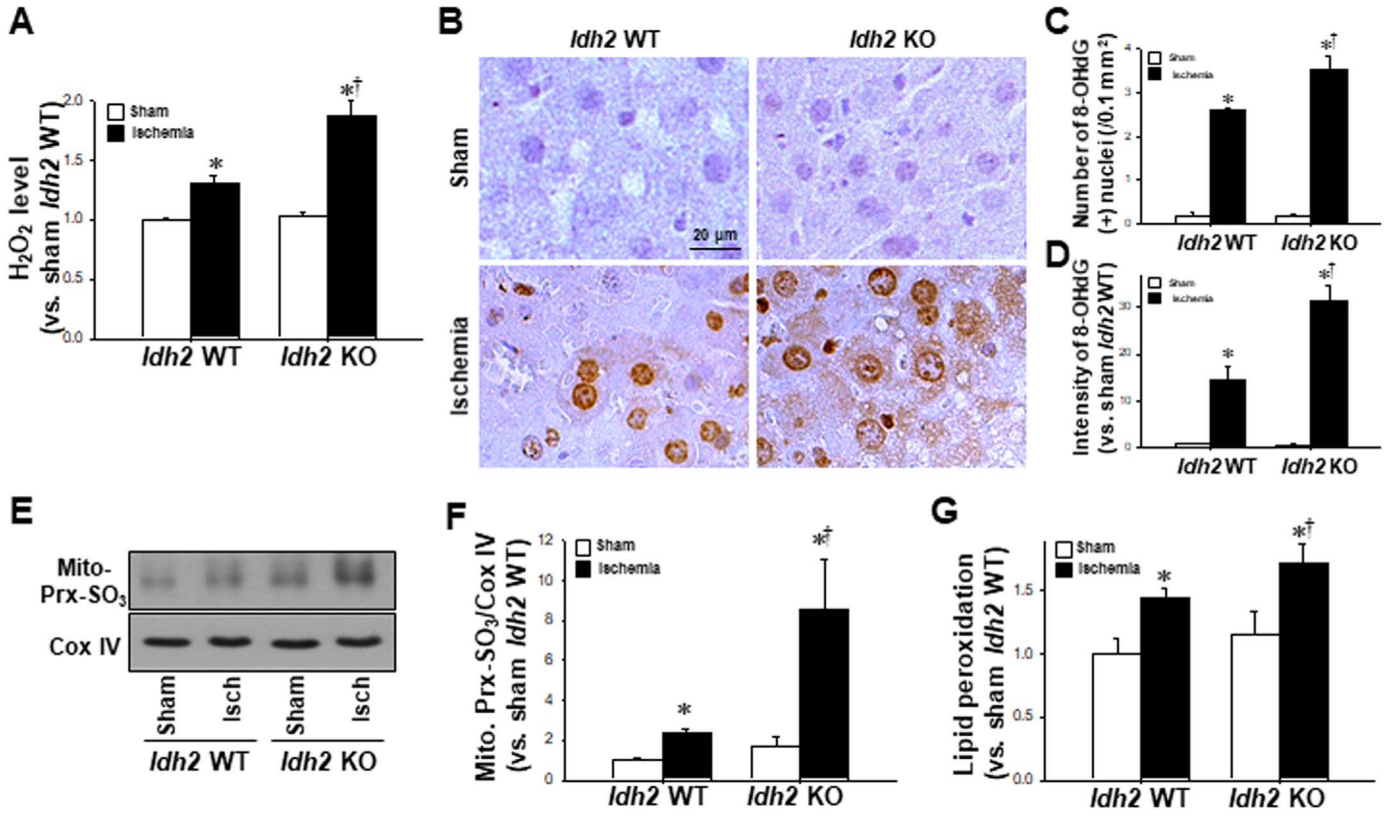

Fig. 4. Levels of reactive oxidative species (ROS) and oxidative stress in *Idh2*$^{+/+}$ and *Idh2*$^{-/-}$ mouse livers after HIR. Livers were harvested 5 h after surgery. (A) Hydrogen peroxide formation was determined in the whole liver tissue. (B) Liver sections were subjected to immunohistochemical staining using an anti-8-hydroxy-2′-deoxyguanosine (8-OHdG) antibody. (C, D) The number of 8-OHdG positive cells and the intensity of 8-OHdG staining were measured. (E) Liver mitochondrial fractions were subjected to western blot analysis using an anti-oxidized peroxiredoxin (Prx-SO_3) antibody. Cox IV was used as the mitochondrial loading control. (F) The density of the Prx-SO_3 band on the blot was determined using ImageJ software. (G) Lipid peroxidation was determined in the whole liver tissue. The results are expressed as the means ± SEM (n = 6). *, $p < 0.05$ vs. respective sham-operated mice. †, $p < 0.05$ vs. ischemia-operated *Idh2*$^{+/+}$. IDH2, mitochondrial NADP$^+$-dependent isocitrate dehydrogenase 2.

2.7. Measurement of the oxidized glutathione (GSSG) to total glutathione ratio in the liver

The ratio GSSG to total glutathione (GSH + GSSG) was measured using an enzymatic recycling method, as described previously [23,24].

2.8. Measurement of enzyme activities and ATP levels

The activities of IDH2, glucose-6-phosphate dehydrogenase (G6PD), and catalase were measured as described previously [25]. The ATP levels were measured using an ATP Colorimetric/Fluorometric Assay Kit (Abcam), according to the manufacturer's instructions.

2.9. Terminal deoxynucleotidyl transferase dUTP nick-end labeling (TUNEL) assay

The TUNEL assay was performed using an in situ cell death detection kit (Fluorescein, Roche Molecular Biochemicals, Indianapolis, IN), according to the manufacturer's instructions. TUNEL-positive cells were counted in 10 fields per liver.

2.10. Transmission electron microscopy (TEM)

One and five hours after ischemia or sham operations, livers were perfusion-fixed via the abdominal aorta with 2.5% glutaraldehyde, and then stored overnight in the fixative at 4 °C. Samples were cut into 1 mm^3 cubes, washed in 0.1 M phosphate buffer, and then post-fixed in aqueous 2% OsO4 for 1.5 h. After three 0.1 M phosphate buffer washes, the samples were dehydrated through a graded series of 50–100% ethanol and 100% propylene oxide. The samples were then infiltrated with 1:1, 1:2, and 1:3 mixtures of propylene oxide:Epon® Resin 828 (Polysciences Inc, Warrington, PA) for 1 h each. After samples had been incubated in 100% Epon® Resin 828 for over 8 h, they were embedded in molds, and cured at 35 °C and 45 °C for 12 h, followed by additional hardening at 60 °C for 2 days. Ultrathin (60 nm) sections were double stained with 2% uranyl acetate and 1% lead citrate. Sections were photographed under a transmission electron microscope (H-7000, Hitachi, Japan) at 75 kV. Electron micrographs of mitochondria were captured from hepatocytes near the central vein. The mitochondrial aspect ratio [(major axis)/(minor axis)], the extent of mitochondrial abnormal enlargement, and the loss of cristae were determined using 30 mitochondria per cell.

2.11. Statistical analysis

Results are expressed as means ± SEM. Statistical differences among groups were calculated using Student's *t*-test and two-way analysis of variance (ANOVA) for comparison between two groups. A p value of < 0.05 was regarded as statistically significant.

3. Results

3.1. Idh2 gene deficiency worsens HIRI

In order to evaluate whether *Idh2* gene deletion affects HIR injury, *Idh2* knockout (*Idh2*$^{-/-}$) and wild-type (*Idh2*$^{+/+}$) littermates were subjected to 60 min of partial hepatic ischemia followed by 5 h of reperfusion (HIR). HIR induced severe histological and functional damage to the livers of both *Idh2*$^{+/+}$ and *Idh2*$^{-/-}$ mice, as reflected by the disruption in liver structure (Fig. 1A, B) and increased plasma AST

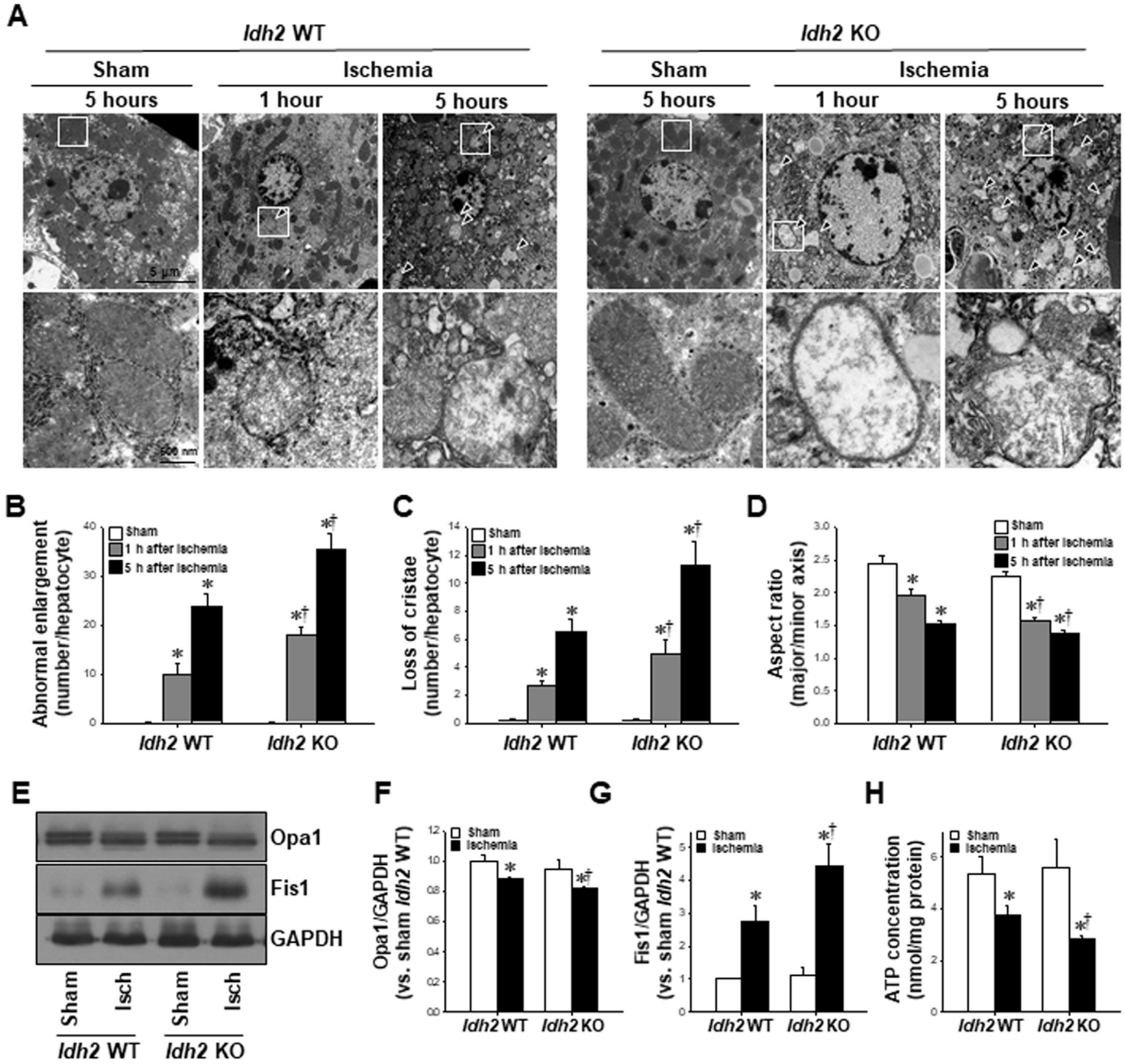

Fig. 5. Mitochondrial fragmentation and damage in the *Idh2*$^{+/+}$ and *Idh2*$^{-/-}$ mouse livers after HIR. Livers were harvested 1 h or 5 h after surgery. (A) Mitochondrial structures were evaluated under a transmission electron microscope (TEM). Upper panels are at low magnification. Lower panels are at high magnification and are the regions that are within the rectangular box in the upper panels. The extent of mitochondrial abnormal enlargement (B) and loss of cristae (C) were measured. (D) The mitochondrial aspect ratio [(major axis) to (minor axis)] was measured. (E) Livers samples 5 h after surgery were subjected to western blot analysis using anti-Optic atrophy 1 (Opa1) and Fission 1 (Fis1) antibodies. GAPDH was used as a loading control. (F, G) Densities of the bands on the blots were measured using ImageJ software. (H) Five hours after surgery, ATP levels were measured. The results are expressed as the mean ± SEM (n = 6). *, $p < 0.05$ vs. respective sham-operated mice. †, $p < 0.05$ vs. ischemia-operated *Idh2*$^{+/+}$. IDH2, mitochondrial NADP$^+$-dependent isocitrate dehydrogenase 2.

(Fig. 1C) and ALT concentrations (Fig. 1D). Furthermore, HIR significantly increased the number of F4/80-positive cells (a marker protein for monocytes/macrophages) in the interstitial area of the liver (Fig. 1E, F). Moreover, HIR increased the expression of Ly6G, a marker protein for neutrophils, in the liver (Fig. 1G, H). These functional and histological changes and the increased inflammation after HIR were greater in the *Idh2*$^{-/-}$ mice than those in the *Idh2*$^{+/+}$ mice (Fig. 1A–H). However, there were no significant differences in plasma ALT and AST, liver structure, and the expression of F4/80 and Ly6G in the liver between sham-operated *Idh2*$^{-/-}$ and sham-operated *Idh2*$^{+/+}$ mice (Fig. 1A–H). These results indicate that *Idh2* gene deletion increased the susceptibility of liver to HIR insult.

3.2. HIR impairs the mitochondrial IDH2-NADPH producing system in the liver

To determine whether HIR affects the mitochondrial IDH2-NADPH producing system, we evaluated the expression and activity of IDH2 in the liver after HIR. First, we determined the effects of the *Idh2* knockout and HIR on the expression and activity of IDH2 in the liver. *Idh2* gene deletion reduced IDH2 expression to nearly non-detectible levels (Fig. 2A, B). Similarly, *Idh2* knockout reduced IDH2 activity to

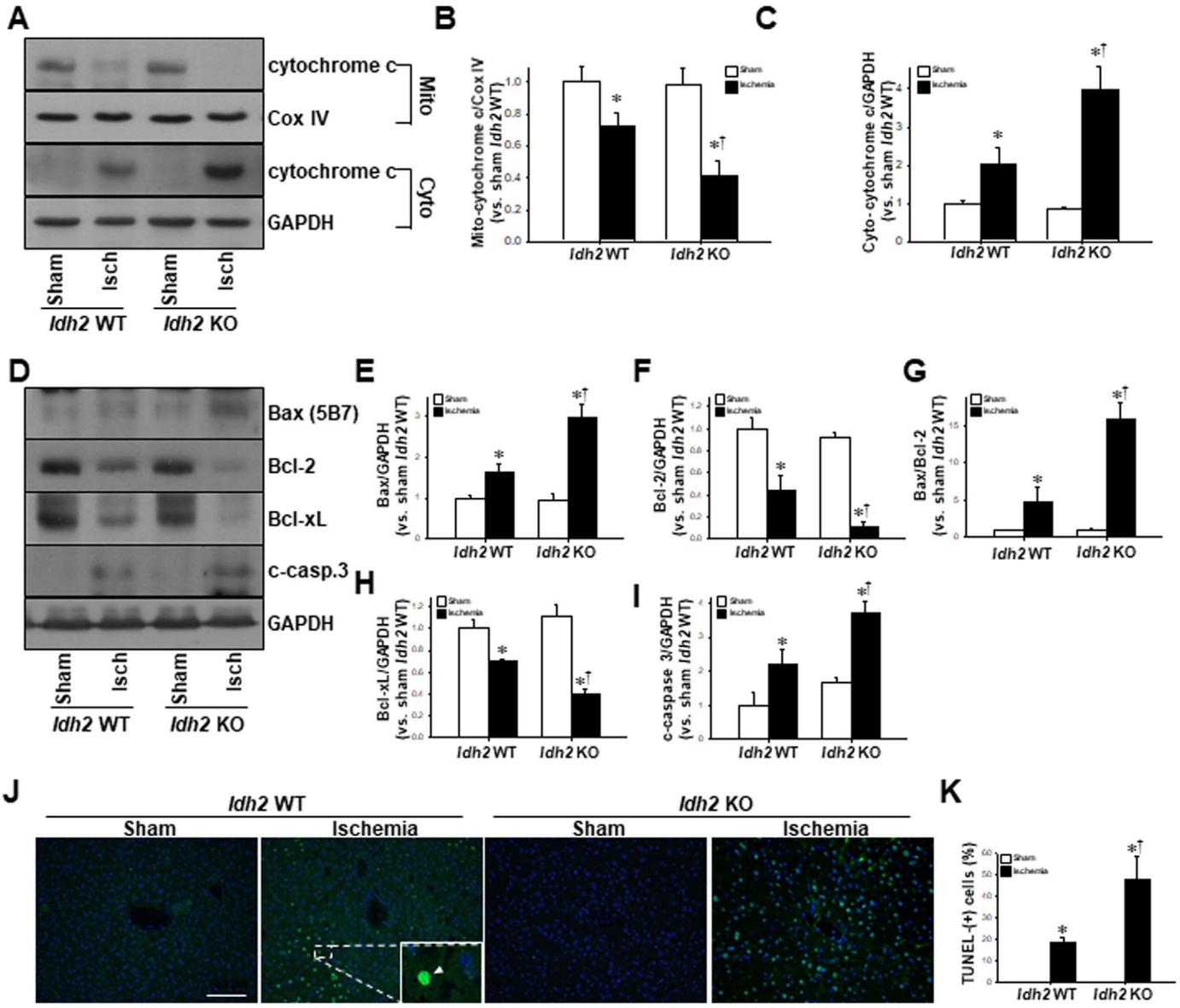

Fig. 6. Apoptosis in the livers of *Idh2*$^{+/+}$ and *Idh2*$^{-/-}$ mice after HIR. Livers were harvested 5 h after surgery. (A) Liver mitochondrial (Mito) and cytosolic (Cyto) fractions were subjected to western blot analysis using an anti-cytochrome *c* (cyto-c) antibody. COX IV and GAPDH were used as loading controls for mitochondrial and cytosolic fractions, respectively. (B, C) The densities of the bands were measured using ImageJ software. (D) Whole liver tissue samples were analyzed by western blot using anti-Bax, -Bcl2, -Bcl-xL, and -cleaved caspase-3 (c-casp. 3) antibodies. GAPDH was used as a loading control. (E to I) The densities of the bands were measured using ImageJ software. (J) Apoptotic cell death was evaluated using a terminal deoxynucleotidyl transferase dUTP nick-end labeling (TUNEL) assay. Arrows (green) in box indicate TUNEL-positive cells. DAPI (blue) was used to stain the nuclei. (K) TUNEL-positive cells were counted. The results are expressed as the mean ± SEM (n = 6). *, $p < 0.05$ vs. respective sham-operated mice. †, $p < 0.05$ vs. ischemia-operated *Idh2*$^{+/+}$. IDH2, mitochondrial NADP$^+$-dependent isocitrate dehydrogenase 2; DAPI, 4′,6-diamidino-2-phenylindole. (For interpretation of the references to color in this figure legend, the reader is referred to the web version of this article).

negligible levels in the whole lysate and mitochondrial fraction of the liver of sham-operated *Idh2*$^{-/-}$ mice and *Idh2*$^{+/+}$ mice (Fig. 2C). The presence of both the mitochondrial and cytosolic fractions was confirmed by COX IV and GADPH expression, respectively; COX IV was detected in the mitochondrial fraction, whereas GAPDH was detected in the cytosolic fraction (Fig. 2D). HIR significantly decreased the IDH2 expression and activity in *Idh2*$^{+/+}$ mice, but IDH2 expression and activity was almost non-detectible in *Idh2*$^{-/-}$ mice (Fig. 2A–C). Next, we examined whether *Idh2* gene deletion and HIR affect NADPH production in the liver. NADPH production was significantly reduced in the post-HIR livers of both *Idh2*$^{-/-}$ and *Idh2*$^{+/+}$ mice compared with that in livers of the sham-operated mice (Fig. 2E, F). This HIR-induced decrease in NADPH was much greater in the *Idh2*$^{-/-}$ mice than in the wild-type littermates (Fig. 2E, F). The NADPH level in the liver of sham-operated *Idh2*$^{-/-}$ mice was lower than that in the liver of sham-operated *Idh2*$^{+/+}$ mice (Fig. 2E, F). Taken together, these data indicate that HIR causes IDH2 dysfunction and that IDH2 deficiency exacerbates HIR-induced impairments including a decrease in NADPH production.

3.3. HIR impairs the mitochondrial GSH antioxidant system

NADPH plays an important role in the GSH-associated antioxidant system by helping to reduce GSSG to GSH, and given this role, it is considered a critical agent in a cell's fight against oxidative stress. Given this information, we first investigated the effects of *Idh2* gene deletion and HIR on the mitochondrial GSH-associated antioxidant system. The ratio of GSSG to total glutathione (tGSH, GSSG + GSH) in the mitochondria increased after HIR and this increase was greater in the *Idh2*$^{-/-}$ mice than the *Idh2*$^{+/+}$ mice (Fig. 3A). However, there were no differences in the ratio of GSSG to tGSH between sham-operated *Idh2*$^{+/}$

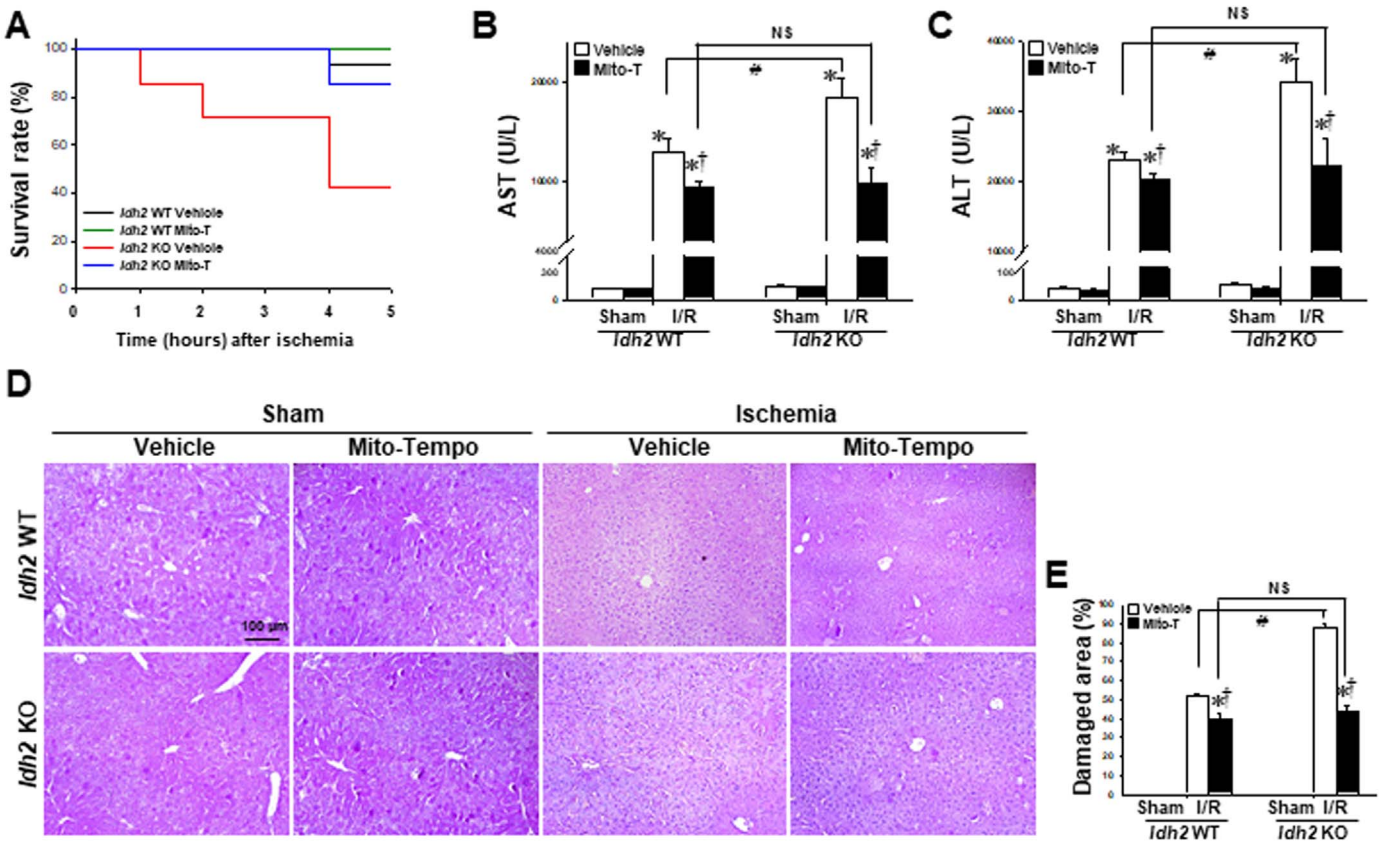

Fig. 7. Effect of Mito-TEMPO treatment on the survival rate, and functional and morphological damage to the livers of *Idh2*$^{+/+}$ and *Idh2*$^{-/-}$ mice after HIR. Mice were treated with mito-TEMPO (mito-T), twice, 17 h and 1 h before either hepatic ischemia or sham-operation and livers were harvested 5 h after surgery. (A) Cumulative survival rates were determined until 5 h after HIR. Data are expressed as the cumulated survival rates (B, C) Five hours after surgery, plasma concentrations of AST (B) and ALT (C) were determined. (D, E) Liver sections were stained with PAS reagent and the damaged areas were evaluated. The results are expressed as the mean ± SEM. *, $p < 0.05$ vs. respective sham-operated mice. †, $p < 0.05$ vs. respective vehicle-I/R. #, $p < 0.05$. NS, no significance.

$^{+}$ and *Idh2*$^{-/-}$ mice (Fig. 3A). Since GR catalyzes the reduction of GSSG to GSH by using NADPH, we next determined whether the *Idh2* knockout and HIR affects GR activity in the mitochondria of liver cells. HIR significantly decreased GR activity and this decrease was greater in the *Idh2*$^{-/-}$ mice than in the *Idh2*$^{+/+}$ mice (Fig. 3B). However, GR activity in the sham-operated *Idh2*$^{-/-}$ mice was not significantly different from that in the sham-operated *Idh2*$^{+/+}$ mice (Fig. 3B). The activity of GPx, which catalyzes the reaction of GSH and H_2O_2 and consequently removes H_2O_2, significantly decreased in the liver mitochondria for both *Idh2*$^{-/-}$ and *Idh2*$^{+/+}$ mice after HIR, and this decrease was greater in the *Idh2*$^{-/-}$ mice than the *Idh2*$^{+/+}$ mice (Fig. 3C). These results suggest that IDH2 is associated with the HIR-induced increases in mitochondrial oxidative injury by impairing the GSH-associated antioxidant system in the mitochondria.

To evaluate whether *Idh2* knockout affects the cytosolic NADPH-GSH system, we determined the effects of HIR and *Idh2* gene deletion on the cytosolic IDH2-NADPH-GSH antioxidant system. HIR induced an increase in the ratio of GSSG to tGSH (Fig. 3D), and decreases in the activities of GR (Fig. 3E) and GPx (Fig. 3F) in the both *Idh2*$^{-/-}$ and *Idh2*$^{+/+}$ mice. However, these levels did not differ between *Idh2*$^{-/-}$ and *Idh2*$^{+/+}$ mice (Fig. 3A–F), suggesting that IDH2 has a critical role in mitochondria rather than in the cytosol. Furthermore, we determined the activity of G6PD, a major NADPH-generating enzyme, in the cytosol [26], and catalase, a major H_2O_2-scavenging enzyme, in the cell [27]. HIR decreased the activity of G6PD (Fig. 3G) and catalase (Fig. 3H), however, there were no significant differences in the activities of G6PD and catalase between *Idh2*$^{+/+}$ and *Idh2*$^{-/-}$ mice. This suggests that *Idh2* gene deletion may not influence the cytosolic antioxidant systems including GPx, GR, G6PD, and catalase activities.

3.4. *Idh2* gene deletion augments mitochondrial oxidative stress after HIR

To further confirm that the impairment in the NADPH-GSH antioxidant system affects hepatocyte oxidative stress, we measured 1) the H_2O_2 level in the whole lysate, 2) protein oxidation by oxidized peroxiredoxin (Prx-SO_3, a well-known indicator of oxidative damage) [28] in the mitochondrial fraction, 3) lipid oxidation, as indicated by MDA production in the whole lysate, and 4) DNA oxidation by the intracellular expression pattern of 8-hydroxy-2′-deoxyguanosine (8-OHdG). Here, we found that HIR led to the increases in H_2O_2 levels (Fig. 4A), 8-OHdG-positive signals (Fig. 4B–D), Prx-SO_3 expression (Fig. 4E, F), and MDA levels (Fig. 4G) in both *Idh2*$^{+/+}$ and *Idh2*$^{-/-}$ mouse liver, and these increases were greater in the *Idh2*$^{-/-}$ mice than those in the wild-type littermates (Fig. 4A–E). Taken together, these data indicate that a defect in IDH2 exacerbates HIR-induced oxidative injuries including increasing the oxidation of lipids, proteins, and DNA.

3.5. *Idh2* knockout exacerbates mitochondrial injury after HIR

To confirm whether defects of the IDH2-NADPH-GSH-GPx system after HIR and IDH2 knockout affect mitochondrial injury, we evaluated the morphology of mitochondria by TEM at 1 and 5 h after HIR. TEM images indicated swelling, cristae loss, and fragmentation of mitochondria in the hepatocytes of both *Idh2*$^{+/+}$ and *Idh2*$^{-/-}$ mice at both time points, with the condition worsening at 5 h post-reperfusion (Fig. 5A–D). Furthermore, the TEM images revealed that mitochondrial damage was most severe in the *Idh2*$^{-/-}$ mice as compared to that in the *Idh2*$^{+/+}$ mice (Fig. 5A–D), indicating that mitochondria of *Idh2*$^{-/-}$ mouse hepatocytes are more susceptible to HIR than those of the *Idh2*$^{+/}$

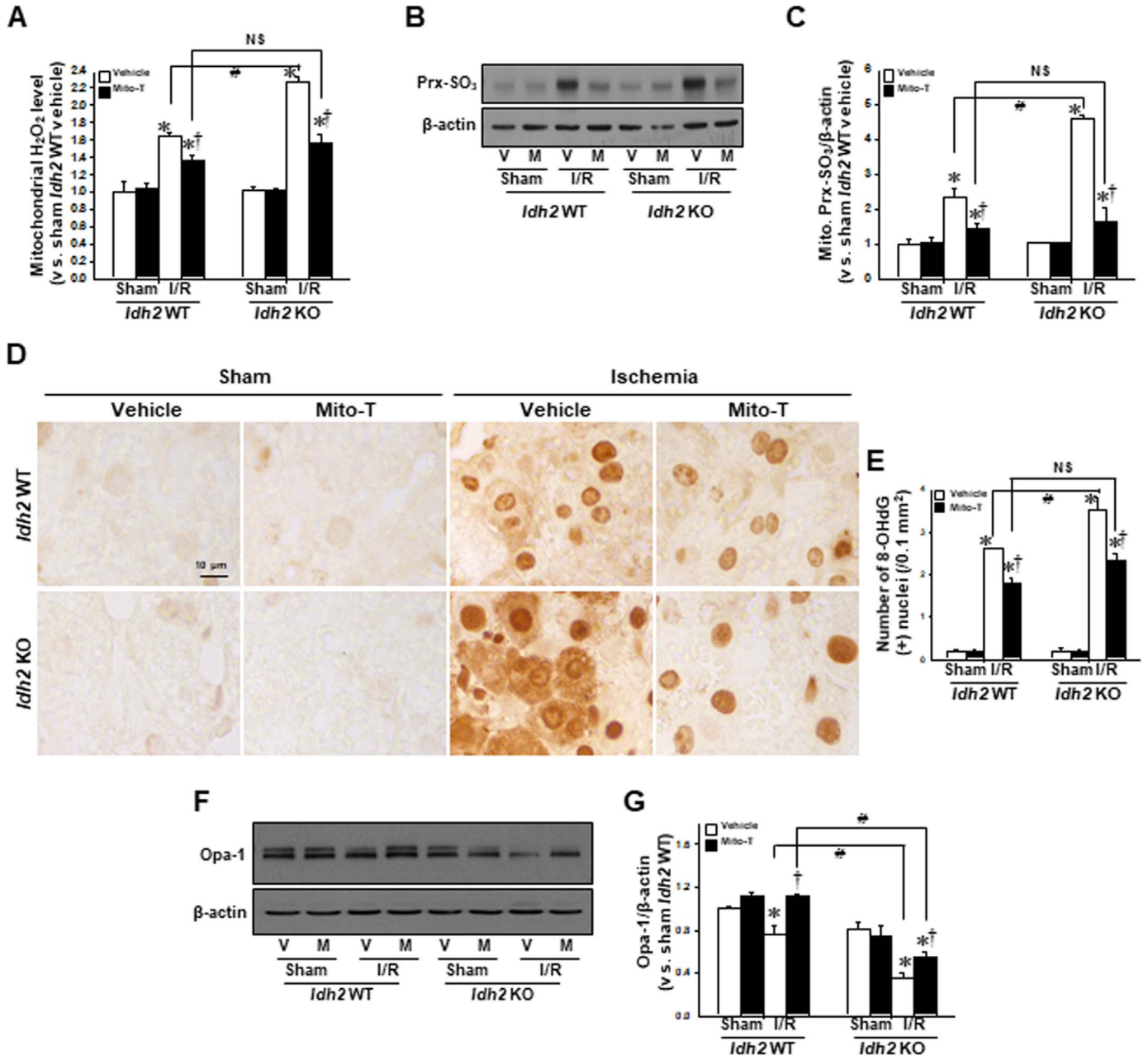

Fig. 8. Effect of Mito-TEMPO treatment on H_2O_2 formation, morphological oxidative damage, and expression of Opa1 and Fis1 in the livers of *Idh2*$^{+/+}$ and *Idh2*$^{-/-}$ mice after HIR. Mice were treated with mito-TEMPO (mito-T), twice, 17 h and 1 h before either hepatic ischemia or sham-operation and livers were harvested 5 h after surgery. (A) Levels of H_2O_2 (I) was measured in mitochondrial fraction. (B, C) Liver mitochondrial fractions were subjected to western blot analysis using an anti-Prx-SO_3 antibody. (C) The density of the Prx-SO_3 band was determined using ImageJ software. (D) Liver sections were subjected to immunohistochemical staining using an anti-8-OHdG antibody. (F) Liver whole lysates were subjected to western blot analysis using an anti-optic atrophy 1 (Opa1) antibody. GAPDH was used as a loading control. (G) Densities of the bands on the blots were measured using ImageJ software. The results are expressed as the mean ± SEM. *, $p < 0.05$ vs. respective sham-operated mice. †, $p < 0.05$ vs. respective ischemia-operated *Idh2*$^{+/+}$.

$^{+}$ mice. Here, we also found that HIR shifted mitochondria into fission as reflected by a decreased aspect ratio (the length of major axis to minor axis) (Fig. 5A, D). This shift was greater in the *Idh2*$^{-/-}$ mice than in the *Idh2*$^{+/+}$ mice (Fig. 5A, D). In addition, we found that HIR decreased the expression of mitochondrial dynamin like GTPase (Opa1, a mitochondrial fusion protein), whereas it increased the expression of fission 1 (Fis1, a mitochondrial fission protein) (Fig. 5E–G), and these HIR-induced changes were greater in the *Idh2*$^{-/-}$ mice than in the *Idh2*$^{+/+}$ mice (Fig. 5E–G). However, we did not find any significant differences in the morphology, aspect ratio, and expression of Opa1 and Fis1 between sham-operated *Idh2*$^{-/-}$ and *Idh2*$^{+/+}$ mouse livers (Fig. 5A–G).

When mitochondrial ATP production was assessed, we found that HIR decreased ATP levels significantly in both *Idh2*$^{+/+}$ and *Idh2*$^{-/-}$ mice (Fig. 5H). These decreases were greater in the *Idh2*$^{-/-}$ mice than in the *Idh2*$^{+/+}$ mice (Fig. 5H). However, we did not find any significant differences in the ATP levels between sham-operated *Idh2*$^{-/-}$ and *Idh2*$^{+/+}$ mouse livers (Fig. 5H). These data indicate that *Idh2* gene deletion exacerbates liver susceptibility to HIR.

3.6. *Idh2* gene deletion exacerbates apoptosis

Typically, mitochondrial damage stimulates apoptotic signaling pathways [29]. Therefore, we evaluated whether IDH2 deficiency and HIR influence the activation of apoptosis. We found that the expression of cytochrome *c* in the mitochondrial fraction of liver lysate decreased in both *Idh2*$^{+/+}$ and *Idh2*$^{-/-}$ mice after HIR, whereas the expression of

cytochrome *c* in the cytosolic fractions increased in both *Idh2*$^{+/+}$ and *Idh2*$^{-/-}$ mice (Fig. 6A–C). Furthermore, we found that the release of cytochrome *c* was greater for the *Idh2*$^{-/-}$ mice than the *Idh2*$^{+/+}$ mice (Fig. 6A–C). This indicates that HIR induces cytochrome *c* release from the mitochondria into the cytosol and *Idh2* gene deletion augments this process. In addition, we found that HIR increased pro-apoptotic factors, Bax and cleaved-caspase 3 (c-casp. 3), in both *Idh2*$^{+/+}$ and *Idh2*$^{-/-}$ mice (Fig. 6D–I). Conversely, HIR suppressed the expression of anti-apoptotic factors Bcl-2 and Bcl-xL in both *Idh2*$^{+/+}$ and *Idh2*$^{-/-}$ mice (Fig. 6D–I). These post-HIR increases in pro-apoptotic factors and decreases in anti-apoptotic factors were greater in the *Idh2*$^{-/-}$ mice than in the *Idh2*$^{+/+}$ mice after HIR injury (Fig. 6D–I). Additionally, HIR increased TUNEL-positive cells in the livers of both *Idh2*$^{+/+}$ and *Idh2*$^{-/-}$ mice, and these increases were greater in the *Idh2*$^{-/-}$ mice than in the *Idh2*$^{+/+}$ mice (Fig. 6J, K). These results indicate that *Idh2* gene deletion exacerbates HIR-induced apoptosis.

3.7. mito-TEMPO, a mitochondria-targeted antioxidant, mitigates HIR-induced liver injury and this mitigation is greater in Idh2 gene-deleted mice than in Idh2 wild type mice

In order to confirm that the increased susceptibility of *Idh2* knockout mice to HIRI is due to a reduction in mitochondrial antioxidant capacity, we tested whether mito-TEMPO, a mitochondria-targeted antioxidant molecule [17], mitigates the increased susceptibility due to *Idh2* deletion. Mito-TEMPO treatment dramatically increased survival rates in both mice and this survival rate increase was greater in the *Idh2*$^{-/-}$ mice than in the *Idh2*$^{+/+}$ mice. Specifically, the survival rates increased from ~ 42% to ~ 85% for *Idh2*$^{-/-}$ mice and from ~ 93% to 100% for *Idh2*$^{+/+}$ mice (Fig. 7A). Moreover, mito-TEMPO treatment mitigated post-HIR increases in AST and ALT concentrations and reduced the histological damage in both *Idh2*$^{-/-}$ and *Idh2*$^{+/+}$ mice, and these mitigations in the *Idh2*$^{-/-}$ mice (about 50% mitigation in histological damage score) were greater than those in the *Idh2*$^{+/+}$ mice (about 20% mitigation in histological damage score) (Fig. 7B–E).

In addition, mito-TEMPO significantly inhibited HIR-induced increases in mitochondrial H_2O_2 levels (Fig. 8A), Prx-SO_3 expression (Fig. 8B, C), and 8-OHdG-positive cells (Fig. 8D, E) in both *Idh2*$^{-/-}$ and *Idh2*$^{+/+}$ mice. Again, these inhibitory effects of mito-TEMPO were significantly greater in the *Idh2*$^{-/-}$ mice than in the *Idh2*$^{+/+}$ mice (Fig. 8A–E); Reductions in cisplatin-induced mitochondrial H_2O_2 production by mito-TEMPO treatment were about 30% in the *Idh2*$^{-/-}$ mice and about 17% in the *Idh2*$^{+/+}$ mice (Fig. 8A); Prx-SO_3 expressions after mito-TEPMO were also dramatically reduced (about 64% in the *Idh2*$^{-/-}$ mice and about 38% in the *Idh2*$^{+/+}$ mice) (Fig. 8B). Furthermore, changes in mitochondrial dynamics (i.e., the shift to fission) after HIR were more dramatically inhibited by mito-TEMPO treatment in the *Idh2*$^{-/-}$ mice than in the *Idh2*$^{+/+}$ mice (Fig. 8F, G). These data indicate that the increased susceptibility of *Idh2* gene-deleted mice to hepatic injury is associated with the increased mitochondrial oxidative stress due to impairments in the mitochondrial antioxidant system. In conclusion, we suggest that HIR-induced hepatic cell damage is associated with impairments in the IDH2-NADPH-GSH axis and that IDH2 is critical for the maintenance of the mitochondrial redox state.

4. Discussion

In the present study, we report, for the first time, that HIR impairs the function of IDH2, leading to defects in the mitochondrial NADPH-GSH antioxidant systems, eventually resulting in mitochondrial oxidative stress, mitochondrial dysfunction, mitochondrial damage, the activation of apoptosis, and cell death. In addition, *Idh2* gene deficiency exacerbates HIR-induced mitochondrial oxidative stress and hepatic dysfunction and cell death. Furthermore, a mitochondria-targeting antioxidant treatment attenuates HIR-induced liver damage and this attenuation was greater in the *Idh2* knockout mice than in wild-type littermates. These results indicate that HIR injury is associated with the impairment of the IDH2-NADPH-GSH antioxidant system and that IDH2 is a critical part of mitochondrial antioxidant defense. Given these results, IDH2 could be considered a novel therapeutic target for HIR-induced liver failure.

Mitochondria inevitably produce ROS due to leakage from the electron transport chain during oxidative phosphorylation, and consequently this increases the production of superoxide radicals. Under normal conditions, the superoxide radicals in mitochondria are converted into H_2O_2 via MnSOD and H_2O_2 is further degraded to H_2O by GPx (about 70–80% of H_2O_2) [30]. However, pathological conditions such as ischemia-reperfusion induces not only excessive ROS production but also defects in the antioxidant systems, leading to increased oxidation of proteins, lipids, and nucleic acids. These effects invariably lead to mitochondrial dysfunction and damage [30]. Furthermore, H_2O_2 generated in mitochondria affect other intracellular organelles and surrounding cells. In mitochondria, GPx removes most of the H_2O_2 via oxidizing GSH to form GSSG, which is subsequently reduced by GR that uses NADPH as the electron donor. In mitochondria, IDH2 catalyzes the reduction of $NADP^+$ to NADPH and is therefore a major provider of NADPH to GPx, glutathione, and Trx/Prx systems for peroxide detoxification [31,32]. It has been reported that IDH2 dysfunction impairs mitochondrial redox balance, leading to a shift toward a more oxidized state where there is an increase in oxidative damage to mitochondrial components, mitochondrial membrane disruption, activation of apoptosis, and eventually cell death [9,12–14]. Evidence has shown that the pathogenesis of HIR injury is associated with excessive mitochondrial ROS generation that overwhelms the mitochondria's antioxidant defense [5,33].

In the present study, HIR causes a reduction in IDH2 expression and activity, leading to a decrease in NADPH levels, an increase in GSSG/GSH, a decrease of GPx activity, and an increase in H_2O_2 levels. Overall, these changes increase oxidative stress within the mitochondria and increases lipid, protein, and DNA oxidation. Thus, it appears that HIR-induced liver damage is associated with reduced IDH2 function. Supporting this, in the present study, knockout of *Idh2* exacerbated HIR-induced mitochondrial oxidative stress and increased mitochondrial damage and dysfunction. Furthermore, treatment with the mitochondria-targeted antioxidant, mito-TEMPO, 17 h prior to and at the beginning of HIR protected mitochondria and the liver cells, and this protection was greater in the *Idh2* gene-deleted mice than in wild-type littermates. A previous study by Okatani et al. supported these results, as they determined that ischemia-reperfusion in the liver decreases mitochondrial GPx activity and causes mitochondrial disorganization, and that antioxidant treatment prevents these HIR-induced injuries [34]. In addition, Mukhopadhyay et al. reported that mitochondrial antioxidants, such as Mito-Q and Mito-CP, ameliorated HIR-induced apoptotic cell death and liver dysfunction by reducing mitochondrial damage and inflammatory responses [5].

Although we cannot provide an exact answer as to how HIR decreases IDH2 function and expression, it is clear that the two are closely linked. A possible answer may stem from HIR-induced mitochondrial oxidative stress, but further studies would be needed to define the exact molecular mechanisms as to how HIR induces IDH2 dysfunction.

Mitochondrial damage such as alterations in mitochondrial membrane integrity, fragmentation, and dysfunction, activate the release of pro-apoptotic substances such as cytochrome *c* and AIF from the mitochondrial intermembrane space into the cytoplasm, and this leads to the activation of apoptosis signaling pathways [35,36]. Oishi et al. reported that HIR induces apoptosis of hepatocytes by producing oxygen free radicals, and antioxidants effectively inhibit apoptosis and protect the liver against HIR insult [37]. Moreover, Frank et al. reported that mitochondrial oxidative stress disrupts mitochondrial membrane integrity, inducing the release of cytochrome *c*, and activating apoptosis in hepatocytes [38]. Consistent with these reports, the present study demonstrated that HIR-induced mitochondrial structural injury and

cytochrome *c* release were exacerbated in *Idh2* knockout mice. This indicates that IDH2 plays an important role in preventing mitochondria-associated apoptotic signaling events via maintaining mitochondrial redox balance.

Recently it has been reported that mitochondrial oxidative stress by ROS and ischemia-reperfusion induces a shift in mitochondria toward fission, which eventually leads to fragmentation [39]. Under normal physiological conditions, the fission and fusion of mitochondria are tightly regulated [40]. Excessive fission of mitochondria precedes cytochrome *c* release and subsequent apoptosis. Zhang et al. reported that the inhibition of fission due to the inhibition of Drp-1, a fission inducing protein, protects liver cells against apoptosis after HIR [41]. Furthermore, it has been reported that Drp-1 assists Bax in assembling into large ring-like structures in the mitochondrial outer membrane to facilitate the release of pro-apoptotic proteins such as cytochrome *c* from the mitochondria into the cytoplasm [42,43]. In addition, Frank et al. reported that the release of cytochrome *c* further promotes mitochondrial fission [38]. Moreover, recently it has been reported that DrP-1 and ROS stress activate mitophagy, a selective form of autophagy in mitochondrial degradation; autophagy aggravates hepatic ischemia-reperfusion injury [44], whereas inhibition of autophagy alleviates hepatic ischemia-reperfusion [45]. In the present study, HIR shifts mitochondria towards fission (as evidenced by an increased aspect ratio, increased Fis1 expression, and decreased Opa1 expression), along with increased cytochrome *c* release into the cytosol, and apoptosis. These HIR-induced alterations were much greater in the *Idh2*$^{-/-}$ mice than in the wild-type littermates. It indicates that mitochondrial oxidative stress after HIR shifts mitochondrial dynamics into fission, which can activate apoptosis in hepatocytes. Further supporting this is the fact that a mitochondria-targeting antioxidant treatment prevents the increase of Fis1 expression and mitochondrial fission, which is accompanied by decreased liver dysfunction and mortality in mice. Furthermore, the protective effects of a mitochondria-targeting antioxidant were more prominent in the *Idh2*$^{-/-}$ mice than in the wild-type littermates.

Taken together, our results demonstrate that HIR impairs the IDH2-associated mitochondrial antioxidant system, resulting in mitochondrial oxidative stress, disruption of mitochondrial function, activation of apoptosis, and overall liver dysfunction. This suggests that IDH2 may be a critical enzyme for maintaining mitochondrial redox balance and may be a useful target protein for the development of therapeutics against liver injury.

Conflict of interest

None declared.

Acknowledgement

This study was supported by the National Research Foundation of Korea (NRF) Grant (NRF- 2015R1A2A1A15052400 and 2017R1A2A2A05069707), funded by the Korean government.

References

[1] M. Elias-Miro, M.B. Jimenez-Castro, J. Rodes, C. Peralta, Current knowledge on oxidative stress in hepatic ischemia/reperfusion, Free Radic. Res. 47 (2013) 555–568.
[2] W. Zhang, M. Wang, H.Y. Xie, L. Zhou, X.Q. Meng, J. Shi, et al., Role of reactive oxygen species in mediating hepatic ischemia-reperfusion injury and its therapeutic applications in liver transplantation, Transplant. Proc. 39 (2007) 1332–1337.
[3] S. Zeng, Y. Lin, J.F. Di, Z. Feng, Protective effect of N-acetylcysteine on liver and lung in mice after ischemia-reperfusion injury, Xi Bao Yu Fen Zi Mian Yi Xue Za Zhi 25 (2009) 1058–1060.
[4] K.H. Moon, B.L. Hood, P. Mukhopadhyay, M. Rajesh, M.A. Abdelmegeed, Y.I. Kwon, et al., Oxidative inactivation of key mitochondrial proteins leads to dysfunction and injury in hepatic ischemia reperfusion, Gastroenterology 135 (2008) 1344–1357.
[5] P. Mukhopadhyay, B. Horvath, Z. Zsengeller, S. Batkai, Z. Cao, M. Kechrid, et al., Mitochondrial reactive oxygen species generation triggers inflammatory response and tissue injury associated with hepatic ischemia-reperfusion: therapeutic potential of mitochondrially targeted antioxidants, Free Radic. Biol. Med. 53 (2012) 1123–1138.
[6] S. Marchi, C. Giorgi, J.M. Suski, C. Agnoletto, A. Bononi, M. Bonora, et al., Mitochondria-ros crosstalk in the control of cell death and aging, J. Signal Transduct. 2012 (2012) 329635.
[7] O.W. Griffith, A. Meister, Origin and turnover of mitochondrial glutathione, Proc. Natl. Acad. Sci. USA 82 (1985) 4668–4672.
[8] M. Mari, A. Morales, A. Colell, C. Garcia-Ruiz, J.C. Fernandez-Checa, Mitochondrial glutathione, a key survival antioxidant, Antioxid. Redox Signal. 11 (2009) 2685–2700.
[9] S.H. Jo, M.K. Son, H.J. Koh, S.M. Lee, I.H. Song, Y.O. Kim, et al., Control of mitochondrial redox balance and cellular defense against oxidative damage by mitochondrial NADP+-dependent isocitrate dehydrogenase, J. Biol. Chem. 276 (2001) 16168–16176.
[10] Z.J. Reitman, H. Yan, Isocitrate dehydrogenase 1 and 2 mutations in cancer: alterations at a crossroads of cellular metabolism, J. Natl. Cancer Inst. 102 (2010) 932–941.
[11] J. Swierczynski, M. Zelewski, S. Zolnierowicz, J. Klimek, J. Marszalek, L. Zelewski, Isolation, properties and role in progesterone biosynthesis of cytosolic malic enzyme from human term placenta, Placenta 8 (1987) 175–184.
[12] E.S. Yang, J.W. Park, Regulation of ethanol-induced toxicity by mitochondrial NADP(+)-dependent isocitrate dehydrogenase, Biochimie 91 (2009) 1020–1028.
[13] I.S. Kil, S.W. Shin, H.S. Yeo, Y.S. Lee, J.W. Park, Mitochondrial NADP+-dependent isocitrate dehydrogenase protects cadmium-induced apoptosis, Mol. Pharmacol. 70 (2006) 1053–1061.
[14] A.H. Shin, I.S. Kil, E.S. Yang, T.L. Huh, C.H. Yang, J.W. Park, Regulation of high glucose-induced apoptosis by mitochondrial NADP+-dependent isocitrate dehydrogenase, Biochem. Biophys. Res. Commun. 325 (2004) 32–38.
[15] H.J. Kim, B.S. Kang, J.W. Park, Cellular defense against heat shock-induced oxidative damage by mitochondrial NADP+ -dependent isocitrate dehydrogenase, Free Radic. Res. 39 (2005) 441–448.
[16] S. Kim, S.Y. Kim, H.J. Ku, Y.H. Jeon, H.W. Lee, J. Lee, et al., Suppression of tumorigenesis in mitochondrial NADP(+)-dependent isocitrate dehydrogenase knock-out mice, Biochim. Biophys. Acta 1842 (2014) 135–143.
[17] A.E. Dikalova, A.T. Bikineyeva, K. Budzyn, R.R. Nazarewicz, L. McCann, W. Lewis, et al., Therapeutic targeting of mitochondrial superoxide in hypertension, Circ. Res. 107 (2010) 106–116.
[18] H.S. Jang, J. Kim, K.Y. Kim, J.I. Kim, M.H. Cho, K.M. Park, Previous ischemia and reperfusion injury results in resistance of the kidney against subsequent ischemia and reperfusion insult in mice; a role for the Akt signal pathway, Nephrol. Dial. Transplant. 27 (2012) 3762–3770.
[19] J. Kim, Y.M. Seok, K.J. Jung, K.M. Park, Reactive oxygen species/oxidative stress contributes to progression of kidney fibrosis following transient ischemic injury in mice, Am. J. Physiol. Ren. Physiol. 297 (2009) F461–F470.
[20] S.J. Han, J.I. Kim, J.W. Park, K.M. Park, Hydrogen sulfide accelerates the recovery of kidney tubules after renal ischemia/reperfusion injury, Nephrol. Dial. Transplant. 30 (2015) 1497–1506.
[21] J.A. Buege, S.D. Aust, Microsomal lipid peroxidation, Methods Enzymol. 52 (1978) 302–310.
[22] C. Frezza, S. Cipolat, L. Scorrano, Organelle isolation: functional mitochondria from mouse liver, muscle and cultured fibroblasts, Nat. Protoc. 2 (2007) 287–295.
[23] T.P. Akerboom, H. Sies, Assay of glutathione, glutathione disulfide, and glutathione mixed disulfides in biological samples, Methods Enzymol. 77 (1981) 373–382.
[24] M.E. Anderson, Determination of glutathione and glutathione disulfide in biological samples, Methods Enzymol. 113 (1985) 548–555.
[25] K. Nakahira, J.A. Haspel, V.A. Rathinam, S.J. Lee, T. Dolinay, H.C. Lam, et al., Autophagy proteins regulate innate immune responses by inhibiting the release of mitochondrial DNA mediated by the NALP3 inflammasome, Nat. Immunol. 12 (2011) 222–230.
[26] M.D. Cappellini, G. Fiorelli, Glucose-6-phosphate dehydrogenase deficiency, Lancet 371 (2008) 64–74.
[27] D.P. Jones, L. Eklow, H. Thor, S. Orrenius, Metabolism of hydrogen peroxide in isolated hepatocytes: relative contributions of catalase and glutathione peroxidase in decomposition of endogenously generated H2O2, Arch. Biochem. Biophys. 210 (1981) 505–516.
[28] T. Rabilloud, M. Heller, F. Gasnier, S. Luche, C. Rey, R. Aebersold, et al., Proteomics analysis of cellular response to oxidative stress. Evidence for in vivo overoxidation of peroxiredoxins at their active site, J. Biol. Chem. 277 (2002) 19396–19401.
[29] K. Sun, Z.S. Liu, Q. Sun, Role of mitochondria in cell apoptosis during hepatic ischemia-reperfusion injury and protective effect of ischemic postconditioning, World J. Gastroenterol. 10 (2004) 1934–1938.
[30] A. Kezic, I. Spasojevic, V. Lezaic, M. Bajcetic, Mitochondria-targeted antioxidants: future perspectives in kidney ischemia reperfusion injury, Oxid. Med. Cell Longev. 2016 (2016) 2950503.
[31] S.J. Han, H.S. Jang, M.R. Noh, J. Kim, M.J. Kong, J.I. Kim, et al., Mitochondrial NADP+-dependent isocitrate dehydrogenase deficiency exacerbates mitochondrial and cell damage after kidney ischemia-reperfusion injury, J. Am. Soc. Nephrol. 28 (2017) 1200–1215.
[32] T. Nakamura, H. Nakamura, T. Hoshino, S. Ueda, H. Wada, J. Yodoi, Redox regulation of lung inflammation by thioredoxin, Antioxid. Redox Signal. 7 (2005) 60–71.
[33] M. Cahova, E. Palenickova, H. Dankova, E. Sticova, M. Burian, Z. Drahota, et al., Metformin prevents ischemia reperfusion-induced oxidative stress in the fatty liver by attenuation of reactive oxygen species formation, Am. J. Physiol. Gastrointest. Liver Physiol. 309 (2015) G100–G111.

[34] Y. Okatani, A. Wakatsuki, H. Enzan, Y. Miyahara, Edaravone protects against ischemia/reperfusion-induced oxidative damage to mitochondria in rat liver, Eur. J. Pharmacol. 465 (2003) 163–170.
[35] S. Elmore, Apoptosis: a review of programmed cell death, Toxicol. Pathol. 35 (2007) 495–516.
[36] A. Hirakawa, N. Takeyama, T. Nakatani, T. Tanaka, Mitochondrial permeability transition and cytochrome c release in ischemia-reperfusion injury of the rat liver, J. Surg. Res. 111 (2003) 240–247.
[37] K. Oishi, S. Hagiwara, S. Koga, S. Kawabe, T. Uno, H. Iwasaka, et al., The vitamin E derivative, EPC-K1, suppresses inflammation during hepatic ischemia-reperfusion injury and exerts hepatoprotective effects in rats, J. Surg. Res. 176 (2012) 164–170.
[38] S. Frank, B. Gaume, E.S. Bergmann-Leitner, W.W. Leitner, E.G. Robert, F. Catez, et al., The role of dynamin-related protein 1, a mediator of mitochondrial fission, in apoptosis, Dev. Cell 1 (2001) 515–525.
[39] J.X. Wang, J.Q. Jiao, Q. Li, B. Long, K. Wang, J.P. Liu, et al., miR-499 regulates mitochondrial dynamics by targeting calcineurin and dynamin-related protein-1, Nat. Med. 17 (2011) 71–78.
[40] L.J. Stallons, J.A. Funk, R.G. Schnellmann, Mitochondrial homeostasis in acute organ failure, Curr. Pathobiol. Rep. 1 (2013).
[41] C. Zhang, J. Huang, W. An, Hepatic stimulator substance resists hepatic ischemia-reperfusion injury by regulating Drp1 translocation and activation, Hepatology (2017).
[42] L. Grosse, C.A. Wurm, C. Bruser, D. Neumann, D.C. Jans, S. Jakobs, Bax assembles into large ring-like structures remodeling the mitochondrial outer membrane in apoptosis, EMBO J. 35 (2016) 402–413.
[43] S. Montessuit, S.P. Somasekharan, O. Terrones, S. Lucken-Ardjomande, S. Herzig, R. Schwarzenbacher, et al., Membrane remodeling induced by the dynamin-related protein Drp1 stimulates Bax oligomerization, Cell 142 (2010) 889–901.
[44] Y. Yu, S. Li, Z. Wang, J. He, Y. Ding, H. Zhang, et al., Interferon regulatory factor-1 activates autophagy to aggravate hepatic ischemia-reperfusion injury via the P38/P62 pathway in mice, Sci. Rep. 7 (2017) 43684.
[45] K. Chen, J.J. Li, S.N. Li, J. Feng, T. Liu, F. Wang, et al., 15-deoxy-delta12,14-prostaglandin J2 alleviates hepatic ischemia-reperfusion injury in mice via inducing antioxidant response and inhibiting apoptosis and autophagy, Acta Pharmacol. Sin. 38 (2017) 672–687.